

INTRODUCTION

The time- and depth-structure maps presented herein are part of an eight-map series of the subsurface of Sabine Peninsula spanning the Early Permian through Early Cretaceous interval. These maps are the product of the application of modern geoscientific methods of processing and interpretation to a suite of legacy seismic-reflection data from onshore Sabine Peninsula (Melville Island, Western Arctic Islands). The resultant processed seismic lines were interpreted using the existing regional geological framework (see Harrison, 1995) by integrating existing regional well data, geophysical settings, age control, and lithological information from original seismicograms.

REGIONAL SETTING

The Sabine Peninsula of Melville Island is located within the Sverdrup Basin in the Queen Elizabeth Islands of the western Arctic. The Sverdrup Basin extends for about 1300 km in a northeast-southwest direction and is up to 350 km wide. The basin contains up to 15 km of sedimentary strata (Embry and Beauchamp, 2008). The Sverdrup Basin is separated from the underlying Franklinian Basin by an unconformity at the base of the Carboniferous strata. The Franklinian Basin was superseded by widespread rifting following the Late Devonian-earliest Carboniferous Ellesmanian Orogeny. The resulting rift-related structural depression acted as a major depocentre from the Carboniferous through the Paleogene (Embry and Beauchamp, 2008). The Sverdrup Basin succession was uplifted and deformed during the early Cenozoic-Eurasian Orogeny.

The surface geology of Melville Island is dominated by Lower Paleozoic strata of the Franklinian Basin. The Sabine Peninsula is an exception to this, as surface strata are part of the Sverdrup Basin. The geology of the Sabine Peninsula consists of deformed Late Carboniferous to Paleocene sandstone, siltstone, shale, and minor amounts of carbonate. Additionally, evaporitic rocks are exposed in two disclines on northern Sabine Peninsula—the Barrow and Colquhoun domes, which consist of deformed anhydrite and gypsum. The strata of the Sverdrup Basin succession on Melville Island were deformed into a series of folds, including the Murray Harbour syncline in the northern part of the peninsula and the Drake Point anticline and the Maryatt Point syncline to the south (Harrison, 1994) (Fig. 1).

During a 1951 to 1955 phase of petroleum exploration, companies drilled 52 wells on Melville Island and surrounding waters (22 of which were on Sabine Peninsula) and acquired about 3,400 line-kilometres of onshore seismic-reflection data (Fig. 2). Three separate gas fields were discovered in the Sabine Peninsula area: Drake Point, Hecta, and Roche Point. Feasibility studies for the development of the gas fields were conducted in the early 1980s; however, due to low gas prices and the lack of gas markets, the gas fields on Melville Island (and elsewhere in the Canadian Arctic) were not developed (Harrison, 1995).

SEISMIC DATA SET AND PROCESSING

Data access was obtained through a Memorandum of Understanding signed in 1997 by the Geological Survey of Canada (GSC), Panarctic Oils, the Arctic Islands Exploration Group, and the offshore Arctic Exploration Group—joint venture parties. The data sets consist of original land seismic-reflection field tapes transcribed from 21-, 7-, and 9-track media. Data were collected using a dynamic charge of 20–30 kg per shot at about 20 m below the surface. Shot-point spacing ranged from 60 m to 300 m, the shorter spacing being used for most surveys. The majority of the seismic-reflection data were recorded using 48- or 96-channel systems. Channel stations were generally deployed using nine receivers spaced at about 6 m and station intervals varying from 50 m to 70 m. The common-midpoint multiplicity of the data sets range from single to 12-fold coverage. The most common recording interval was 8 s.

The processing consisted of three main steps: 1) principal component decomposition was used to remove both coherent and random noise; 2) data were migrated utilizing poststack Kirchhoff migration; and 3) seismic bandwidths were extended to increase vertical resolution (Claproot et al., 2011; Duchesne et al., 2012).

Velocity model

A 3-D velocity model was built using about 1300 km of linear seismic data (78 lines) and 13 wells spread over an area of about 2000 km² (Fig. 2). The velocity model was then used for poststack migration processing and to convert seismic horizon surfaces from time to depth. The primary assumption behind the velocity model is that the coherent high-amplitude reflectors that were picked to build the model correspond to important acoustic impedance contrasts caused by significant and abrupt velocity changes. This assumption was confirmed by tying seismic picks to well sonic logs (Duchesne et al., 2012). The geostatistical approach of kriging with an external drift (KED) was applied to both the reflection time of the picked seismic horizons and time-depth pairs derived from check shot data to compute the 3-D velocity field. Kriging interpolates values between the known positions based on weighted spatial correlations. The KED technique was specifically developed for the integration of seismic data into the kriging process where the number of wells is insufficient for the computation of adequate depth statistics (Hass and Dubrule, 1994). Hence, it uses the information provided by the time horizon picks to improve estimates where depth control is sparse. For seismic migration, root mean squared (RMS) velocity values are first estimated by KED from time-to-depth conversion of seismic horizon surfaces mapped as important velocity boundaries (Duchesne et al., 2012). Then, once the approximate depths of the surfaces are known, the interval velocities (V_{int}) for all time intervals delimited by two consecutive horizons is computed from:

$$V_{int} = \frac{\Delta z}{\Delta t_i}$$

where z and t are the depth and time intervals between two successive horizons i . Once V_{int} is obtained the RMS velocity (V_{rms}) is calculated using:

$$V_{rms} = \sqrt{\frac{1}{t_0} \sum_{i=1}^N V_{int}^2 \Delta t_i}$$

in which N is the total number of horizons and t_0 is the sum of all time intervals.

SEISMIC INTERPRETATION AND VISUALIZATION METHODS

Processed seismic lines were loaded into IHS Kingdom[®] seismic and geological interpretation software. Prominent seismic-reflection horizons, tied to well formation-top information, were manually correlated. Seed points were generated at seismic line intersections, thereby permitting the interpretation of adjacent lines.

The map would benefit from a detailed structural interpretation; however, confidence of this interpretation is minimized due to minor vertical offsets (about 0.1 s) attributed to faulting and the large line spacing. These reflections are readily identified across faults despite offset.

Time-structure maps of the key seismic horizons were computed using universal kriging. Universal kriging permits the interpretation of a nonstationary, random field by adding a term in the kriging equation that accommodates any linear trends present in a scattered point set (Chilès and Delhomme, 1999). Given that all picked horizons showed a strong linear trend for time versus depth over distance, universal kriging provided the best fit to the picked horizons.

TIME TO DEPTH CONVERSION

All time surfaces are converted to depth using the following procedure. First V_{int} of the 3-D velocity model are calculated using Dix equation:

$$V_{int} = \left[\frac{V^2}{t_n} - \frac{V^2}{t_{n-1}} \right]^{1/2}$$

where t is the zero-offset arrival time of the reflection. Interval limits corresponded to seismic horizons that are picked and tied to geological interfaces. Then V_{int} are extracted from the velocity model along picked horizons. Velocity maps are then computed using Universal Kriging at a cell size of 250 m. Finally, the time-structure surfaces of the various seismic horizons are converted to depth (Z) using:

$$Z = \frac{t_{int}}{2}$$

Because the depth-conversion process is a function of the velocity model, the lateral extent of depth maps is confined to the lateral extent of the model. The final depth-structure maps were imported into ArcGIS for visualization using the Arc extension Team-GIS Kriging.

DESCRIPTIVE NOTES

UNCERTAINTY

Quantifying the uncertainty of seismic subsurface maps is difficult since several sources of data, each with their unique level of uncertainty, are used in the map generation. Sources of error may arise from limitations in acquisition, processing, and interpretation. Moreover, seismic data are collected remotely and the images they provide are derived from generalized mathematical and physical concepts. Constraints in acquisition that increase the uncertainty include gaps in coverage because of obstacles to source and receiver deployment, and effect of direction of shooting on data quality (Sheriff and Geldart, 1995). Processing errors may result from inadequate static corrections, inaccurate velocity analysis, and inappropriate parameter determination.

More specifically to this data set, errors may have also been introduced by the velocity model and the ability to form horizons to seismic horizons. The velocity model represents an estimation of the velocity fluctuations for which the accuracy depends on the number of wells and the good fit between time picks and corresponding depths at the well locations. A regression analysis shows that time picks and their corresponding depths at the wells have a strong linearly ($r = 0.98$), meaning that the use of time picks as the external drift in the kriging strategy is justified and appropriate. Nevertheless, the uncertainty of the velocity increases when the distance between the well and any points where velocity is predicted exceeds the range of the varlogram expressing the space dependence between depth and time. In the present case, the range of the different horizons is between 9.5 km and 34 km. The ability to form horizons to seismic horizons relies on the successful use of well sonic and density logs, since it is the contrast between the product of these properties for two successive geological layers that generates reflections recorded in seismic exploration. Formation tops used in this study are from Dewing and Embry (2007), for which they mainly utilized gamma ray logs to position the upper limit of the formations in depth. Thus errors may have been introduced by projecting the formation tops on seismic sections recorded in time.

TIME- AND DEPTH-STRUCTURE DATA DISPLAY

The time- and depth-structure data shown on this map were gridded at a cell size of 250 m using Universal Kriging. Each map presents a grid with a stretched colour ramp at 20% transparency. Time contours generated from the time-structure grids are shown in black at a 50 ms interval, whereas depth contours derived from the depth-structure grid are presented at 100 m intervals.

INVINCIBLE MAP DESCRIPTIONS

The Early Cretaceous Christopher Formation consists of shale, chert, carbonate, and oolite/breccias (Dewing and Embry, 2007; see also Fig. 3). Formation-top data indicate that the Christopher Formation is underlain exclusively by the Isachsen Formation. The Christopher Formation can be separated into the Macdougall Point and Invincible Point members (Dewing and Embry, 2007).

The mapped Invincible Formation reflection extends from north of Eldridge and Shearwater bays to the Colquhoun Dome at the northern limit of the peninsula, but does not cover the entire width of the peninsula. The data gap west of Eden Bay marks the location of Barrow Dome. Two-way traveltimes of the Invincible Formation reflection increase northwards from 3.7 ms to 10.1 ms, or from 55 m to 1613 m. The slope of the horizon averages 1.5° with the steeper slopes (up to 7°) observed between the Drake Point anticline and the Barrow Dome, aligned roughly parallel to the axis of the Murray Harbour syncline. The primary dip azimuth of the grid is to the north with two exceptions: 1) the area it crosses the Drake Point anticline and Maryatt Point syncline, and 2) the area of northwest dip of the Murray Harbour syncline (Harrison, 1994).

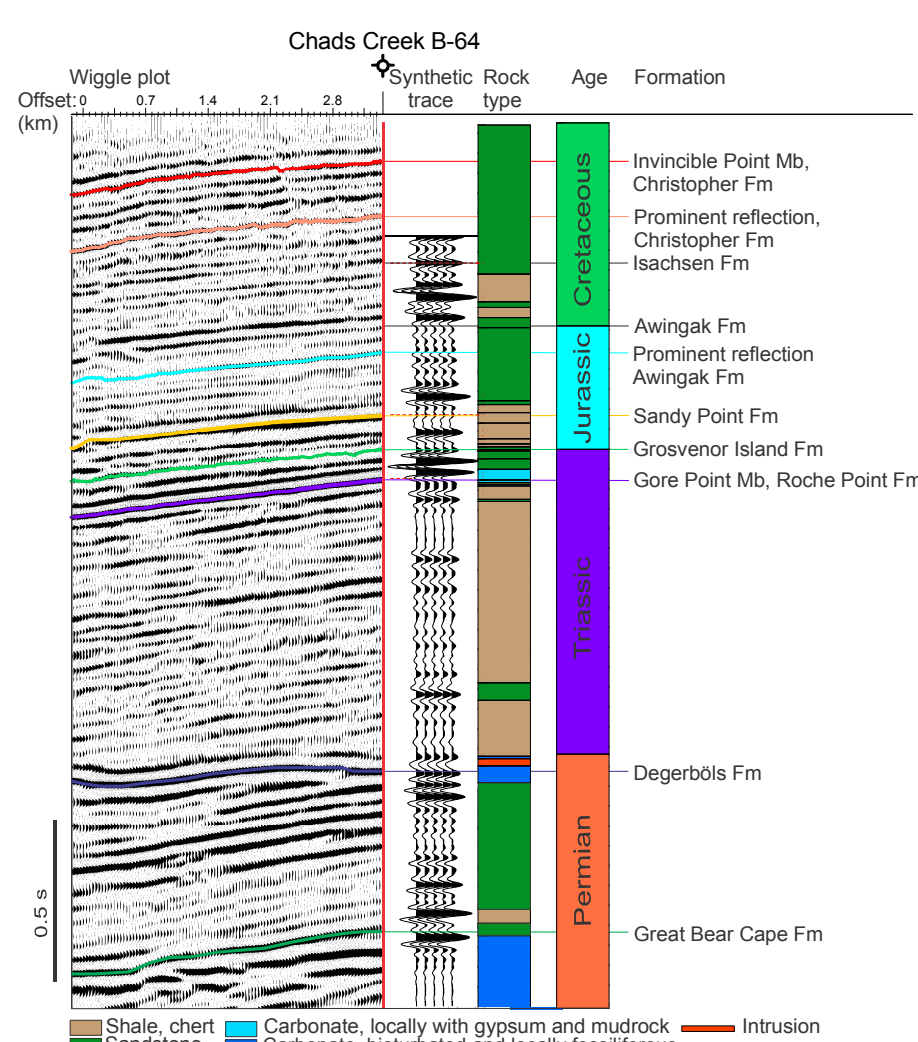


Figure 3. Comparison of the wiggle plot, synthetic trace, stratigraphy, age, and formation-top data for the Chads Creek B-64 well.

ACKNOWLEDGMENTS

The authors would like to thank J. Delinich and B. MacLean (GSC Calgary) for their technical support that improved the overall quality of the maps. IHS is acknowledged for providing Kingdom 8.8 seismic interpretation software.

REFERENCES

- Chiles, J.-P. and Delhomme, P., 1999. Geostatistics: Modeling Spatial Uncertainty. Wiley Series in Probability and Statistics. Wiley, New York, New York, 741 p.
- Claproot, M., Duchesne, M.J., and Glogauer, E., 2011. A geostatistical approach for 2-D seismic velocity modelling. Geological Survey of Canada, Open File 7045, 21 p. doi:10.4095/296551
- Dewing, K. and Embry, A.F., 2007. Geological and geochemical data from the Canadian Arctic Islands. Part 1: Stratigraphic tops from Arctic Islands' oil and gas exploration boreholes. Geological Survey of Canada, Open File 5442, 100 p. doi:10.4095/23389
- Duchesne, M.J., Claproot, M., and Glogauer, E., 2012. Improving seismic velocity estimation for 2-D poststack time migration of regional seismic data using kriging with an external drift. The Leading Edge, v. 31, p. 1159–1166.
- Embry, A. and Beauchamp, B., 2008. Sverdrup Basin. In: Sedimentary Basins of the World, (ed.) K.J. Hult. Volume 5. The Sedimentary Basins of the United States and Canada. Elsevier, Amsterdam, The Netherlands, p. 451–471.
- Harrison, J.C., 1994. Melville Island and adjacent smaller islands. Canadian Arctic Archipelago: District of Franklin, Northwest Territories. Geological Survey of Canada, Map 1544A, scale 1:250 000, doi:10.4095/203577
- Harrison, J.C., 1995. Melville Island's salt-based fold belt. Arctic Canada. Geological Survey of Canada, Bulletin 472, 344 p. doi:10.4095/203576
- Hess, A. and Dubrule, O., 1994. Geostatistical inversion – a sequential method of stochastic reservoir modelling constrained by seismic data. First Break, v. 12, p. 561–568.
- Sheriff, R.E. and Geldart, L.P., 1995. Exploration Seismology. Cambridge University Press, New York, New York, 628 p.

Recommended citation
Brake, V.I., Duchesne, M.J., Dewing, K., Claproot, M., Glogauer, E., and Embry, A.F., 2013. Time- and depth-structure map, Invincible Point Member, Christopher Formation, Sabine Peninsula, Melville Island, Nunavut–Northwest Territories. Geological Survey of Canada, Canadian Geoscience Map 162, scale 1:200 000. doi:10.4095/293086

Authors: V.I. Brake, M.J. Duchesne, K. Dewing, M. Claproot, E. Glogauer, and T.A. Brent
Time-structure map by V.I. Brake and M.J. Duchesne, Geological Survey of Canada, 2013
Depth-structure map by M.J. Duchesne and V.I. Brake, Geological Survey of Canada, 2013
Seismic interpretation by V.I. Brake and M.J. Duchesne, Geological Survey of Canada, 2010–2013

Geomatics by V.I. Brake, Geological Survey of Canada and G. Huot-Vézina, Institut national de la recherche scientifique
Cartography by R. Boivin
Scientific editing by E. Inglis
Initiative of the Geological Survey of Canada, conducted under the auspices of the Western Arctic Islands' project as part of Natural Resources Canada's Geo-mapping for Energy and Minerals (GEM) program.

CANADIAN GEOSCIENCE MAP 162

TIME- AND DEPTH-STRUCTURE MAP
INVINCIBLE POINT MEMBER
CHRISTOPHER FORMATION

Sabine Peninsula, Melville Island
Nunavut–Northwest Territories

1:200 000

Map projection: Universal Transverse Mercator, zone 12
Base map at the scale of 1:250 000 from Natural Resource Canada, with modifications.
Proximity to the North Magnetic Pole causes the magnetic compass to be useless in this area.

The Geological Survey of Canada welcomes corrections or additional data that may include additional observations not portrayed on this map. See documentation accompanying the data.
This publication is available for free download through GEOCAN (http://geocan.nrcan.gc.ca/).
This map is not to be used for navigational purposes.

5 0 5 10 15 20 km



Canadian
Geoscience Maps

Canada